Our measurement of the width for the decay $\phi \rightarrow \rho\pi$ is smaller than values obtained by other experiments.[21] However, the width we measure, $\Gamma(\phi \rightarrow \rho\pi) \approx 0.4$ MeV, when compared to the value $\Gamma(\omega \rightarrow 3\pi) \approx 8.5$ MeV,[23] lends credence to the approximation used in Eqs. (10) that $\epsilon \approx 0$. Our experimental results for the decay $\phi \rightarrow \eta\gamma$ (branching ratio $= 0 \pm 8\%$) agree with the prediction of Eq. (10c) (approximately 8%). However this just means that our experiment is not sensitive enough to confirm or deny the prediction. The determination of the $\eta\gamma$ branching ratio remains an important test of the mixing theory.

[23] The best measurements of the total widths of the ϕ and ω are 3.1 ± 1.0 and 9.5 ± 2.1 MeV, respectively. See N. Gelfand, D. Miller, M. Nussbaum, J. Ratau, J. Schultz, J. Steinberger, T. H. Tan, L. Kirsch, and R. Plano, Phys. Rev. Letters **11**, 438 (1963).

ACKNOWLEDGMENTS

The authors wish to acknowledge the efforts of the scanning and measuring staff, and of the bubble-chamber crews headed by Robert Watt. In particular, we thank Dr. Joseph J. Murray, under whose direction the K^- beam was designed and built, and Professor Luis Alvarez for his support and encouragement in this experiment. We also thank Professor George Trilling for valuable conversations concerning the background in our $\Lambda 3\pi$ sample.

PHYSICAL REVIEW VOLUME 147, NUMBER 4 29 JULY 1966

Search for Dibaryon Resonant States*

E. BIERMAN, A. P. COLLERAINE, AND U. NAUENBERG
Palmer Physical Laboratory
and
Princeton-Pennsylvania Accelerator, Princeton University, Princeton, New Jersey
(Received 3 March 1966; revised manuscript received 13 April 1966)

A search for dibaryon resonant states was carried out in p-p collisions at 5.0 BeV/c in the 80-in. Brookhaven bubble chamber. A total of ~1400 events was measured and analyzed. We were not able to detect any effect which could be construed as being due to a dibaryon resonance. We observed the Y_1^* and the N^{*++} resonance. We also observe the effect of the 1688^{*++} resonance in its $\Lambda^0 K^+$ decay mode. Our data are consistent with the one-pion-exchange model.

RECENTLY, some interest has evolved in the possibility of observing two-baryon resonant states. In the context of the SU_3 symmetry scheme, one of these states might be the isotopic spin doublet ($I = \frac{1}{2}$) member of the $\{10\}^*$ representation of which the deuteron is the singlet ($I = 0$) member. In such a case, the resonant state could decay into a lambda and a proton (Λp) or a sigma and a proton (Σp).[1] Another possibility is that the dibaryon belongs to the $\{27\}$ representation of which the two-nucleon unbound triplet state ($I = 1$) is a member. Work with counter techniques has already indicated the possible existence of such states.[2]

We report here on a search carried out with the 80 in. Brookhaven hydrogen bubble chamber with a beam of 4.95-BeV/c protons.[3] The reactions studies are the following:

(1) $p+p \rightarrow \Lambda^0+p+K^+$,
(2) $p+p \rightarrow \Sigma^0+p+K^+$,
(3) $p+p \rightarrow \Lambda^0+p+K^++(\pi^0)$,
(4) $p+p \rightarrow \Lambda^0+K^++\pi^++(n)$,
(5) $p+p \rightarrow \Lambda^0+\pi^++p+K^0$,
(6) $p+p \rightarrow \Sigma^0+\pi^++p+K^0$,
(7) $p+p \rightarrow \Lambda^0+\pi^++p+(K^0)$,
(8) $p+p \rightarrow K^0+\pi^++p+(\Lambda^0)$,
(9) $p+p \rightarrow K^0+\pi^++p+(\Sigma^0)$,
(10) $p+p \rightarrow \Sigma^++p+K^0$,
(11) $p+p \rightarrow \Sigma^++\pi^++K^0+(n)$,
(12) $p+p \rightarrow \Sigma^++p+K^0+(\pi^0)$,
(13) $p+p \rightarrow \Lambda^0+K^++p+\pi^++\pi^-$,
(14) $p+p \rightarrow K^0+K^++p+(n)$,
(15) $p+p \rightarrow p+p+K^0+\bar{K}^0$.

* This work was supported by the U. S. Atomic Energy Commission.

[1] See, for example, R. J. Oakes, Phys. Rev. **131**, 2239 (1963).

[2] P. A. Piroué, Phys. Letters **11**, 164 (1964), W. J. Hogan, P. F. Kunz, A. Lemonick, P. A. Piroué, and J. S. Smith, Bull. Am. Phys. Soc., **10**, 517 (1965); A. C. Melissinos, N. W. Reay, J. T. Reed, T. Yamanouchi, E. Sacharidis, S. J. Lindenbaum, S. Ozaki, and L. C. L. Yuan, Phys. Rev. Letters **14**, 604 (1965). This latter effect was also observed by W. A. Wenzel. See also G. Alexander, O. Benary, N. Kidron, A. Shapera, R. Yaari, and G. Yekutieli, Phys. Rev. Letters **13**, 355 (1964). The first experiment that studied strange-particle production in p-p collisions at 2.85 BeV was that of R. I. Louttit, T. W. Morris, D. C. Rahm, R. R. Rau, A. M. Thorndike, W. J. Willis, and R. M. Lea. Phys. Rev. **123**, 1465 (1961).

[3] I. Skillicorn and M. S. Webster, Brookhaven National Laboratory Bubble Chamber Report No. DC-H-10 (unpublished).

TABLE I. Measured cross sections.

Reaction	No. of events in fiducial region	No. of events which are ambiguous in fit	Σ^0 background (%)	Neutral V decay correction	Correction due to non-measurable events (%)	Cross section (μb)	O.P.E. model (μb)
$p+p \to p+\Lambda^0+K^+$	173	7	0	3/2	9	48±4	42±6
$p+p \to p+\Sigma^0+K^+$	91	5	0	3/2	8	25±3	
$p+p \to p+\Lambda^0+K^++\pi^0$	112	10	~10	3/2	7	28±3	
$p+p \to n+\Lambda^0+K^++\pi^+$	163	5	~10	3/2	7	41±5	
$p+p \to p+\Lambda^0+\pi^++K^0$	198	13	~10	9/7	4	42±5	
$p+p \to p+\pi^++K^0+\Sigma^0$	36	4	0	3	7	20±3	
$p+p \to p+\Sigma^++K^0$	31	0	0	3	7	17±3	
$p+p \to p+\pi^0+\Sigma^++K^0$	13	0	0	3	7	7±2	
$p+p \to n+\pi^++\Sigma^++K^0$	14	0	0	3	7	7±2	
$p+p \to p+\pi^++K^++\pi^-+\Lambda^0$	24	0	0	3/2	7	7±2	
$p+p \to p+K^++n+\bar{K}^0$	21	4	0	3	7	12±3	
$p+p \to p+p+K^0+\bar{K}^0$	10	0	0	3/2	4	3±1	

The symbols in parentheses indicate here particles not observed in the bubble chamber but required to exist by the kinematics of the reactions.

I. EXPERIMENTAL PROCEDURE

(1) Scanning, Measuring and Analysis

The film was scanned three times in order to have a high scanning efficiency. In the last scan only 40 events were found which were missed previously. We were able to achieve a scanning efficiency of 95%. Each scan was carried out independently in 2 views. All frames where a V was observed were recorded independently of whether or not there was a possible vertex from which the V originated. Those frames where a V without an interaction vertex was present were especially checked in the last scan to make sure no possible vertex could be found. During the scanning, if a V and the interaction vertex from which it originated were found, a picture of the event was taken for use in the analysis of the data.

All recorded events with an observable interaction were measured in three views. Those events where the black spot due to the illumination of the chamber covered either the decay or the interaction vertex in any of the three views were not measured. A correction was made for these events in the cross section determination. The data were then analyzed with the CERN THRESH and GRIND computer programs.[4] The computer programs tried to fit a measured event under various hypotheses, each of which consisted in assigning various mass combinations to the different tracks. Every event was then examined by a physicist. For a hypothesis to be accepted as correctly describing the event, it had to satisfy two requirements: (1) that the probability of the fit was $\geq 1\%$, and (2) that the fit agreed with the ionization as observed in the photographs taken at the scanning table. In approximately 10% of the cases, there were two hypotheses that satisfied these two criteria, and in only a few cases were there more than two. We applied two criteria to these events in order to remove as many ambiguities as possible:

(a) In the case of ambiguities between reactions (1) and (2), the fitted beam momentum on reaction (2) was systematically 30 MeV/c or more higher than the mean while the fitted beam momentum for reaction (1) was distributed about the mean (4.95 BeV/c). For all these cases, we considered the correct hypothesis to be reaction (1).

(b) If ambiguities existed between any two pairs of hypotheses, then the one whose probability of fit was greater than 5 times the probability of the other was accepted as the correct hypothesis.

(2) Determination of the Cross Sections

A beam count was taken every 50 frames. A rectangular fiducial region was chosen between $x=0.0$ cm and $x=126.0$ cm (x is the direction of the beam in the chamber); $y=0.0$ cm and $y=38.0$ cm and all values of z. (z is the depth of the chamber.) The length of every beam track in the frame was measured. If the track interacted within the fiducial region, the length of the track up to the interaction was recorded. In order to obtain the value of the hydrogen density, we counted the number of interactions in our fiducial region for those pictures that were beam counted. We found 5162 interactions and a total beam count of 3.49×10^6 cm of track length. The scanning efficiency was 95±2%. The total cross section for p-p interactions at 4.95 BeV/c is very well known[5]; namely, $\sigma=43.5\pm1.5$ mb. We obtain then for our hydrogen density $\rho=0.061\pm0.002$ g/cm^3. This is in very good agreement with the values obtained from measurements of the vapor pressure of the hydrogen during the exposure, namely, $\rho=0.062$ g/cm^3.[6] Because of the finite size of the chamber and the large

[4] W. G. Moorhead, CERN Report No. 60-33 (unpublished); R. Bock, CERN Report No. 61-29 (unpublished).

[5] T. Fugjii, G. B. Chadwick, G. B. Collins, P. J. Duke, N. C. Hein, M. A. R. Kemp, and F. Turkot, Phys. Rev. 128, 1836 (1962). Previous work on the subject is mentioned here.

[6] A few typical hydrogen density values are given in Ref. 7, p. 8.

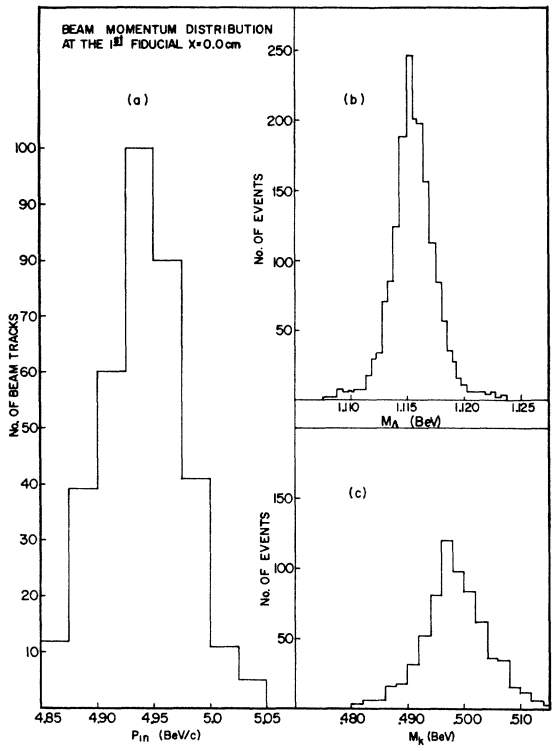

FIG. 1. (a) Beam momentum distribution. (b) Mass distribution of the Λ^0 decay. (c) Mass distribution of the K^0 decay.

possible Λ^0 momentum, we have to apply a correction for those events where the Λ^0 decays outside the chamber volume. This correction is only important for reaction (1) where a 2% correction is applied in the cross section. In addition, a correction of 7% is necessary owing to events not measured because they were not visible in all three views. The purity of the beam in the chamber is essentially 100%. This was determined in two ways: (a) A Čerenkov counter placed in front of the chamber indicated at most 1/100 background due to pions and kaons. (b) A check of delta rays produced by the beam tracks failed to show the presence of any pions or kaons in the beam. The sensitivity of the delta-ray search was 0.1%.

The number of events where in fact a Σ^0 was produced but the event fitted as a Λ^0 production (this effect we will call the Σ^0 background) was surmised in the following way: Reactions (5), (7), and (8) are the same except that in reaction (5) we observe the decay of both the Λ^0 and K^0; in reaction (7) we observe the decay of only the Λ^0 and in reaction (8) we observe the decay of only the K^0. Using the branching ratio of the K^0 and Λ^0 nonvisible decays to all decay modes, we should observe these reactions in the ratio 2:4:1, respectively. The number of observed events in the fiducial region was 49, 122, and 26 events, respectively. The Σ^0 background we assume can be neglected in reactions (5) and (8), since the fitting computer programs tell us when the event is really a Σ^0; namely, reactions (6) and (9) are of this category. Hence, we observe an excess of events in reaction (7) of the order of $(16\pm14\%)$. In addition, we found 3 events which fitted reactions (3), (4), and (7) and where a gamma ray or Dalitz pair was observed [these electron-positron pairs were checked to make sure they did not fit the π^0 decay kinematics in the case of reaction (3)]. This is consistent with a background no larger than 10%. Since in these reactions we have, as we will see, mainly Y_1^* production and since the branching ratio $Y_1^* \to \Sigma^0+\pi/Y_1^* \to \Lambda+\pi$ is very small, we can say that the Σ^0 background is of the order of 10%. In reaction (1) this background is included in the 5 events which are ambiguous in the fit to reaction (2) since they are ambiguous with reaction (1). The measured cross sections are shown in Table I.

(3) Study of the Systematics in the Measurement and Analysis Procedure

The beam momentum as shown in Fig. 1(a) was determined by the measurement of beam tracks using the magnetic field and optical constants as measured at B. N. L.[7] A check on the absolute calibration of the magnetic field was made with the mass distribution of the lambda and kaon as determined from their decay products. This is shown in Figs. 1(b), (c). No deviations from the measured magnetic field were detected. A study

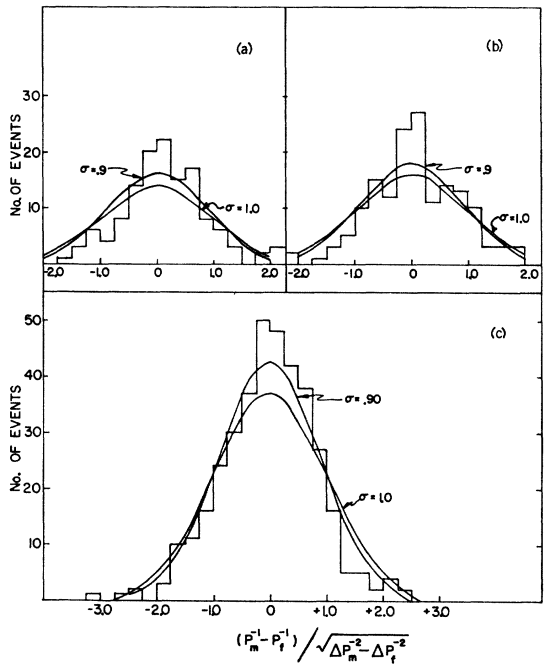

FIG. 2. Distribution of "pulls" in measured quantities, (a) in the production c.m. system for dip measurements; (b) for azimuth measurements; (c) for momentum measurements.

[7] E. L. Hart, Brookhaven National Laboratory Hydrogen Bubble Chamber Internal Report No. BC-04-3-B (unpublished).

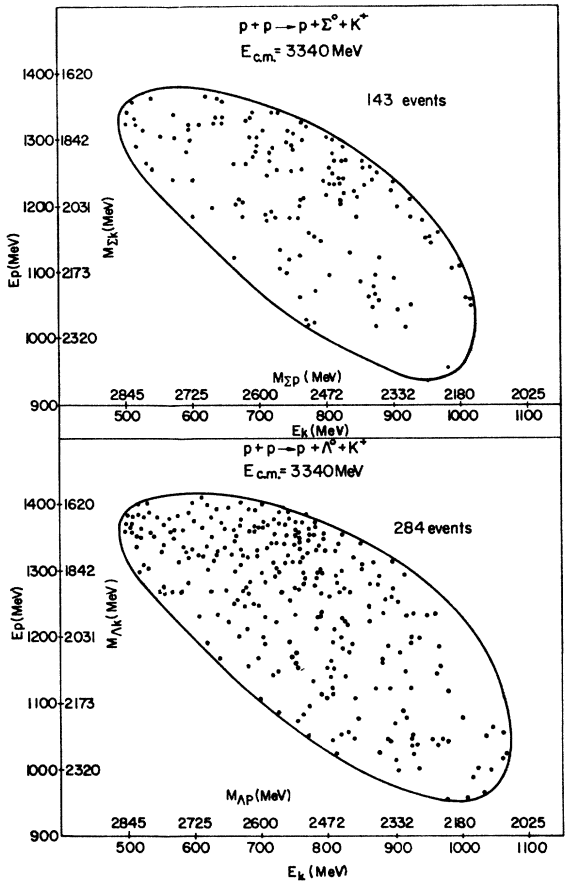

FIG. 3. Dalitz plots for reactions (1) and (2).

of the systematics of the kinematic fitting is shown in Figs. 2(a), (b), (c). Here we plot the "pulls" on the momenta, dip angle, and azimuth angle of the tracks that belong to a correctly fitted event. These distributions are in good agreement with the expected Gaussian distributions except that their half-widths of ~ 0.90[8] is smaller than the expected value of 1.0. This indicates a 10% overestimation in our error assignments.

II. THE DATA ANALYSIS

The Dalitz plots for reactions (1) and (2) are shown in Fig. 3. In both Dalitz plots there is a larger density of events in the region of low kaon-hyperon mass. This is clearly seen in Fig. 4 where the combined mass distribution for the Λ-K and Σ-K systems are shown. We have indicated in these graphs the distributions expected from phase space and the one-pion-exchange model. Clearly, only the one-pion-exchange model describes the data, although a combination of 80% one-pion-exchange process with a 20% nonperipheral phase-space contribution gives just as good a fit to the data (a χ^2 probability of 20%). Similarly, for reaction (2) the one-pion-exchange distribution is in agreement with the data. The one-pion-exchange model whose Feynman diagrams are shown in Fig. 5 predicts that the cross sections should be of the form[9]

$$\frac{d\sigma}{d\Delta^2 d\omega^2} = \frac{1}{8\pi}\frac{G^2}{4\pi}\frac{\sigma(\omega)}{(P_p W)^2}\frac{\Delta^2}{(\Delta^2+M_\pi^2)^2}K\omega,$$

where

$$K=\frac{1}{\omega}\{\tfrac{1}{4}\omega^4-\tfrac{1}{2}\omega^2(M_p^2+M_\pi^2)+\tfrac{1}{4}(M_p^2-M_\pi^2)^2\}^{1/2},$$

$G^2/4\pi$ = pion-nucleon coupling constant ≈ 15,
Δ = four-momentum transfer of the nucleon,
ω = combined mass of the Λ and K,
$\sigma(\omega)$ = cross section for the reaction $\pi^0+p \to \Lambda^0+K^+$ or $\pi^0+p \to \Sigma^0+K^+$,
W = center-of-mass energy of the whole system,
$P_p = (\tfrac{1}{4}W^2-M_p^2)^{1/2}$.

We are neglecting the interference term between the two Feynman graphs. At high energy, these effects are expected to be small. The energy dependence of the cross section for the reaction $\pi^0+p \to \Lambda^0+K^+$ can be related by charge independence to the energy depend-

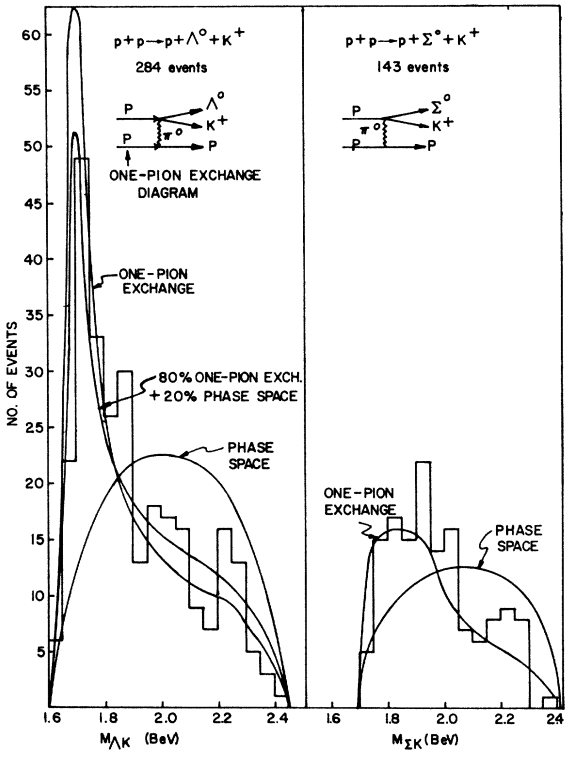

FIG. 4. Mass distribution of the hyperon-kaon system in reactions (1) and (2).

[8] We would like to thank Professor Kehoe from Maryland for a discussion on the correct form of the "pull" quantity.

[9] The one-pion exchange in this reaction is described in many places. See E. Ferrari, Phys. Rev. **120**, 988 (1960); Tsu Yao, *ibid.* **125**, 1048 (1962).

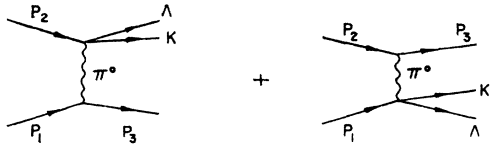

FIG. 5. Feynman diagrams in the one-pion-exchange model.

ence of the reaction $\pi^-+p\rightarrow\Lambda^0+K^0$ namely,

$$\sigma_{\Lambda^0K^+}(\omega)=\tfrac{1}{2}\sigma_{\Lambda^0K^0}(\omega).$$

The reaction $\pi^-+p\rightarrow\Lambda^0+K^0$ has been well studied[10] and we use this to fit the data in Fig. 4. The determination of the cross section for the reaction $\pi^0+p\rightarrow\Sigma^0+K^+$ is not so simple since charge independence gives rise to only a group of inequalities. Nevertheless, since all the reactions where a Σ is produced do not have sharp energy variations, it is reasonable to assume that the energy dependence of the reaction $\pi^0+p\rightarrow\Sigma^0+K^+$ is similar to that for the reaction $\pi^-+p\rightarrow\Sigma^0+K^0$.[11] We have made use of this assumption in the fit to the Σ-K mass distribution. We note also that the measured cross section for reaction (1) is in agreement with the prediction of the one-pion-exchange model. This is shown in Table I.

The very marked deviation from phase space that we observe at $M_{\Lambda K}=1.7$ BeV is due to the fact that the reaction $\pi^-+p\rightarrow\Lambda^0+K^0$ has a resonance at $M=1.69$ BeV.[10] This is the N^* resonance $I=\frac{1}{2}$, $J^P=\frac{5}{2}^+$.[12] (M is also the center-of-mass energy of the π-p system.) It is important to realize, as we will show later, that the marked effect at $M=1.7$ BeV is not only due to the $M=1.69$ BeV resonance; it is more appropriate to consider it as the one pion exchange model effect where N^* resonance gives a small contribution to the cross section $\sigma(\pi^0+p\rightarrow\Lambda^0+K^+)$. It is a fact that the reaction $\pi^-+p\rightarrow\Lambda^0+K^0$ at $M=1.69$ BeV goes not only through the $F_{5/2}$ angular momentum channel but also has contributions from the S and P angular momentum channels which interfere with one another. As we will see, it is more likely that we are observing the effect due to all the contributing channels in the reaction $\pi^0+p\rightarrow\Lambda^0+K^+$ rather than due to the $F_{5/2}$ channel only.

The deviation from phase space of the Σ-K mass combination in reaction (2) is not as marked as in reaction (1). This is due to the fact that the cross section for the reaction $\pi^0+p\rightarrow\Sigma^0+K^+$ as we use it does not have the resonant behavior of the reaction in which a Λ^0 is produced.

In Fig. 6 we show the angular distribution of the proton in the production center-of-mass system for reaction (1). Since we have two identical particles in the incoming channel, the angular distribution is symmetric about $\cos\theta=0$. Therefore, we present only the folded distribution. We note good agreement with the one-pion-exchange model both in the region of the peak ($M_{\Lambda K}<1.9$ BeV) and outside it. The angular distribu-

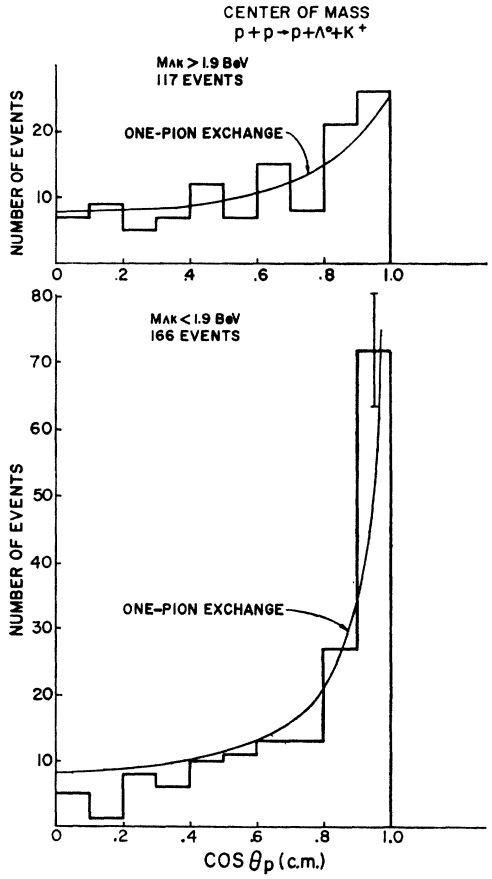

FIG. 6. Angular distribution of the proton in the production c.m. system in reaction (1).

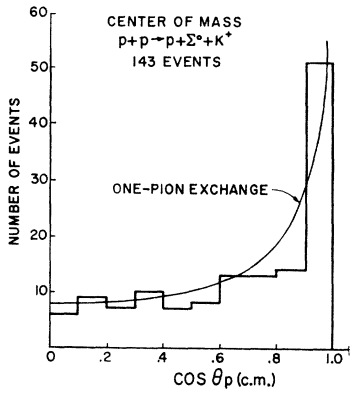

FIG. 7. Angular distribution of the proton in the production c.m. system in reaction (2).

[10] See for example, Joseph Keren, Phys. Rev. 133, B458 (1964) and Nevis Cyclotron Laboratories, Columbia University Report No. 118 (unpublished).

[11] We would like to thank W. A. Wenzel and R. L. Crolius for their data on this reaction.

[12] P. J. Duke, D. P. Jones, M. A. R. Kemp, P. G. Murphy, J. D. Prentice, J. J. Thresher, H. H. Atkinson, C. R. Cox, and K. S. Heard, Phys. Rev. Letters 15, 468 (1965).

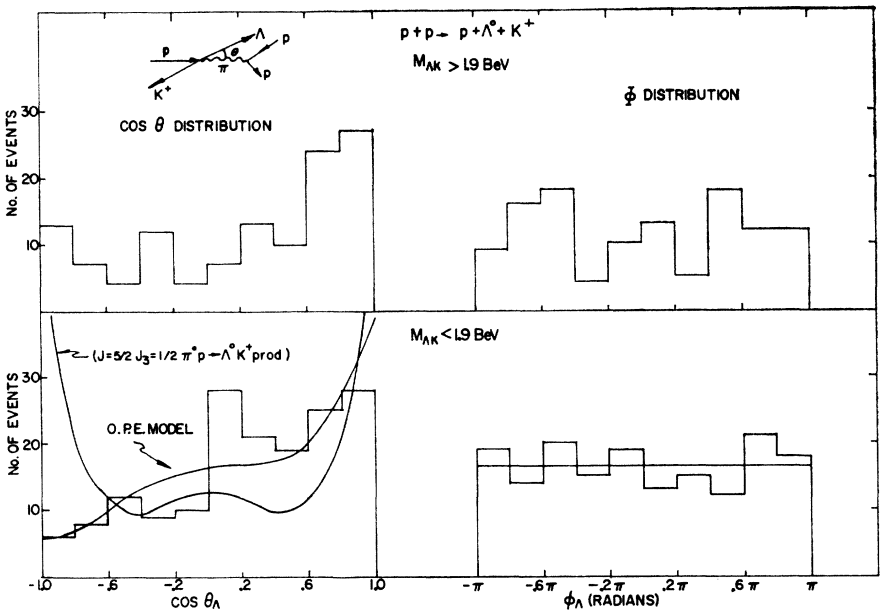

FIG. 8. Plot of the Jackson parameters in reaction (1).

tion for $M_{\Lambda K}<1.9$ BeV tends to be more sharply peaked towards $\cos\theta=1$ than predicted by the one-pion-exchange model. This is what one would expect if some absorption were present[13] in the incoming and outgoing channels.

In Fig. 7 we show the $\cos\theta$ distribution for reaction (2). Again, we have good agreement with the one-pion-exchange model.

In Fig. 8 we show the plot of the "Jackson parameters",[14] both for events in the isobar mass region and outside ($M_{\Lambda K}<1.9$ BeV and >1.9 BeV, respectively). The distribution in ϕ (essentially ϕ in this plot is identical to the Yang-Treiman angle[15]) is flat, which is consistent with the one pion exchange model. The distribution in $\cos\theta$ shows that not all the events in the isobar region go through the resonant $F_{5/2}$ angular momentum channel at the pion-nucleon vertex. In fact, the distribution is most consistent with the one-pion-exchange model. One of the curves shown is the angular distribution of the Λ^0 observed in the reaction $\pi^-+p\rightarrow\Lambda^0+K^0$ at the Σ-K threshold[10] ($M_{\Lambda K}=1.69$ BeV). The agreement with the data is good (with a χ^2 probability of 40%). If all our events in the isobar region were produced through the $F_{5/2}$ channel, then we would expect a distribution in even powers of $\cos\theta$. The data are in disagreement with any distribution consisting only of even powers of $\cos\theta$. For example, using the density-matrix formalism, in the limit that only $\rho^{5/2}{}_{1/2,1/2}$ is not zero (i.e., we neglect absorption effects in the one-pion-exchange[13] model), we would expect a distribution of the form

$$\frac{d\sigma}{d\cos\theta}=\text{const}(5\cos^4\theta-2\cos^2\theta+1).$$

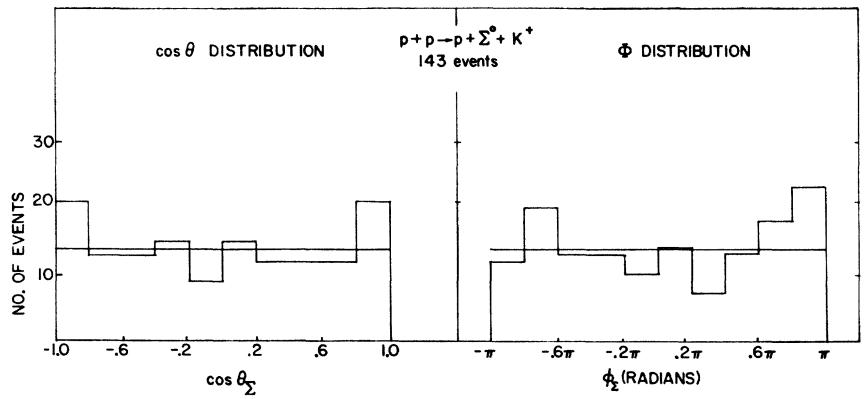

FIG. 9. Plot of the Jackson parameters in reaction (2).

[13] K. Gottfried and J. D. Jackson, Nuovo Cimento 34, 735 (1964). Our notation is $\rho^J{}_{m_J,m_J}$ where $J=$(angular momentum of the resonance) and $m_J=$(Z component of the angular momentum).
[14] J. D. Jackson, Nuovo Cimento 34, 1644 (1964).
[15] S. Treiman and C. N. Yang, Phys. Rev. Letters 8, 140 (1962).

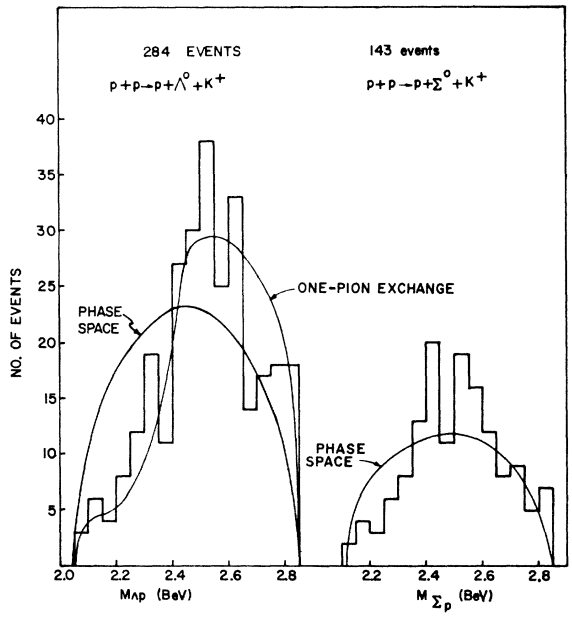

FIG. 10. Mass distribution of the hyperon-nucleon system in reactions (1) and (2).

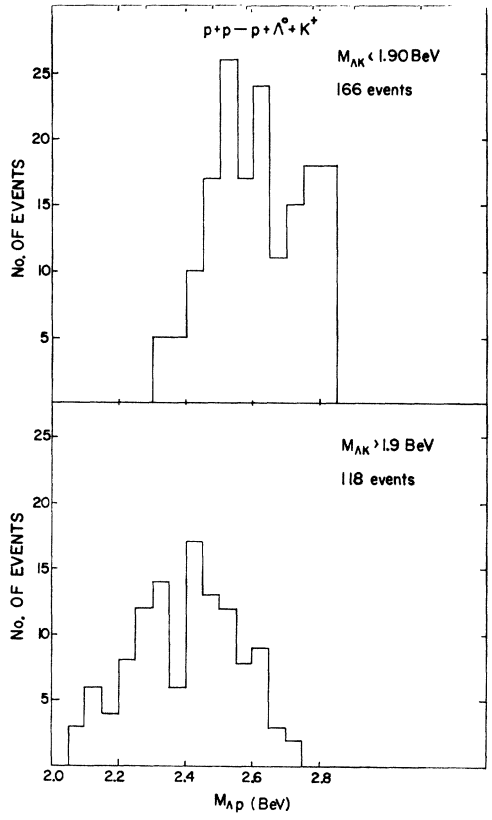

FIG. 11. Mass distribution of the hyperon-nucleon system in reaction (1) for $M_{\Lambda K}<1.9$ BeV and otherwise.

We plot this distribution in Fig. 8 and there is clear disagreement between the data and any distribution of this form. Hence, we can say that more than one angular momentum channel is contributing to reaction (1) at the $\pi^0+p\rightarrow\Lambda^0+K^+$ vertex.

The same plots for reaction (2) are shown in Fig. 9. The distribution in ϕ is flat in agreement with the one-pion-exchange model. We cannot make any comparisons of the $\cos\theta$ distribution with the theory since the angular distribution for the reaction $\pi^0+p\rightarrow\Sigma^0+K^+$ is not known.

In Fig. 10 we show the Λ-p and Σ-p mass distributions. The lack of agreement with phase space is evident. This effect is present for both reactions (1) and (2). These deviations from phase space could be the same as those observed by Piroué[2] in p-p collisions at lower energies. Nevertheless, from the Dalitz plots shown in Fig. 3, we cannot find any evidence that these mass "bumps" are

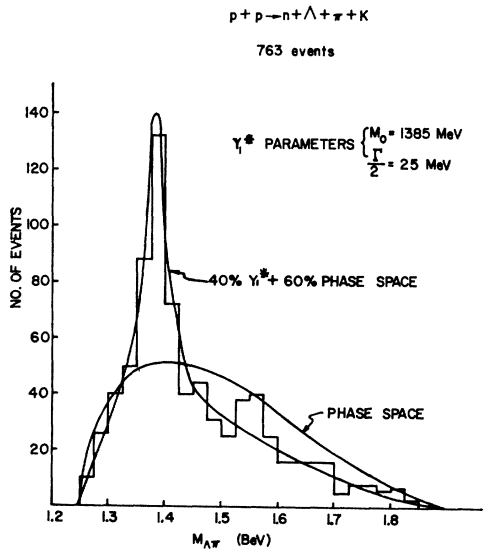

FIG. 12. Mass distribution of the hyperon-pion system in reactions (3), (4), (5), (7), and (8).

manifestations of a resonant state in the usual sense; namely, we find no evidence for a conglomeration of events in a band region with Λp or Σp mass between 2.4 and 2.6 BeV. We have calculated by the Monte Carlo technique the Λp mass distribution expected in the one-pion-exchange model. The curve is plotted in Fig. 10 normalized to the total number of events. The agreement of the data with the one-pion-exchange model is fair (with a χ^2 probability of 15%). In Fig. 11 we show the Λp mass distributions for events with $M_{\Lambda K}<1.9$ BeV and $M_{\Lambda K}>1.9$ BeV. The graphs show that most of events in the Λp mass bump come from the region having $M_{\Lambda K}<1.9$ BeV. If this effect were a resonance uniformly populating a band region in the Dalitz plot, we should expect more events in the region $M_{\Lambda K}>1.9$ BeV than in the region $M_{\Lambda K}<1.9$ BeV. We

can consider then this mass bump as a reflection of the one-pion-exchange model. In the case of reaction (2) we can say that the effect we observe in the Σ-p mass distribution is consistent with the one-pion-exchange model. We cannot calculate what the model predicts since we do not know the $\pi^0+p\rightarrow\Sigma^0+K^+$ angular distribution.

In conclusion, then, all our observed effects for reactions (1) and (2) can be considered as the one-pion exchange being the dominant mechanism by which these reactions take place. We do not observe within our statistics any effect that can be considered as only due to a dibaryon resonance.

The rest of this paper will consist mainly of a discussion of the data where four particles are produced in the final state. In Fig. 12 we show the $\Lambda\pi$ mass distribu-

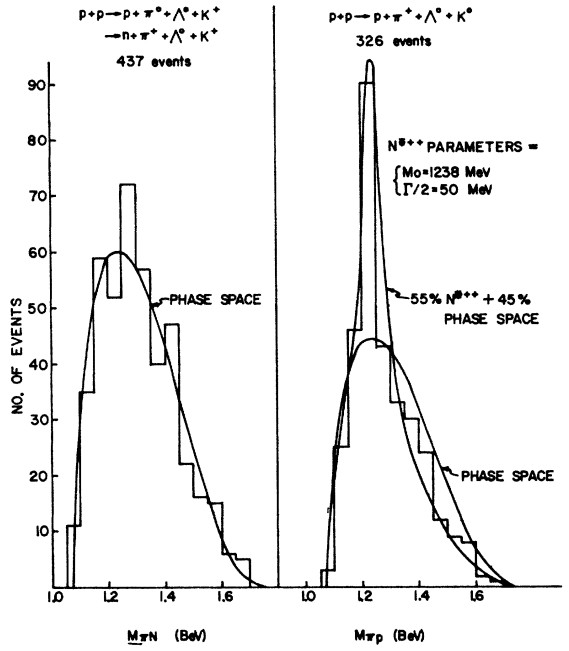

FIG. 13. Mass distribution of the pion-nucleon system in reactions (3) and (4) and separately in reactions (5), (7), and (8).

tion for the combined data of reactions (3), (4), (5), (7), and (8). There is a large relative production cross section of the Y_1* resonance. In addition, in reaction (5), (7), and (8) we also observe the N^{*++} resonance ($I=\frac{3}{2}$, $J^P=\frac{3}{2}^+$) being produced. In Fig. 13 we show the nucleon-pion mass distributions; one mass plot for the $p\pi^+$ mass combination where the N^{*++} is clearly observed and one for the $p\pi^0$ and $n\pi^+$ mass combinations where it is not observed. This is expected since the N^* resonance is produced 9 times more frequently in the $p\pi^+$ channel than in the others. In Fig. 14 we show the $p\pi^+$ mass distributions for events whose $\Lambda\pi^+$ mass value falls within the Y_1* mass ± 60 MeV, and also we show it for those events whose $\Lambda\pi^+$ mass falls outside the Y_1* region. The data indicate that the N^{*++} pro-

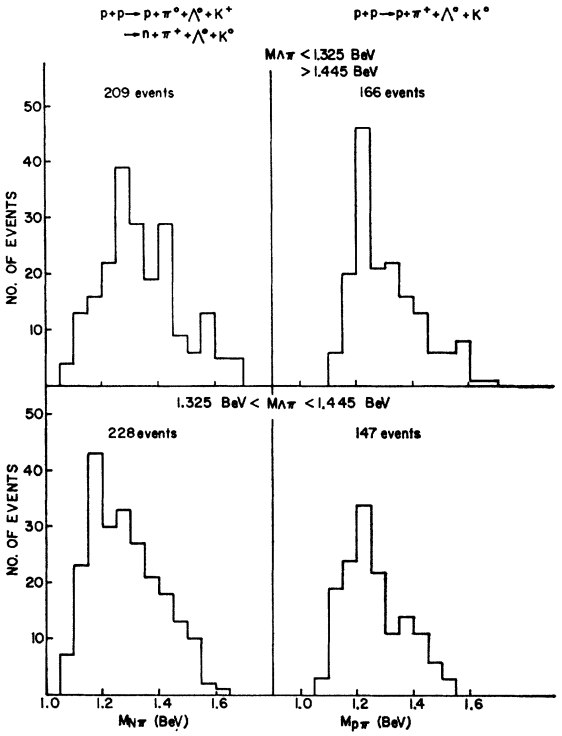

FIG. 14. Mass distribution of the pion-nucleon system for events where a Y_1* is produced and otherwise.

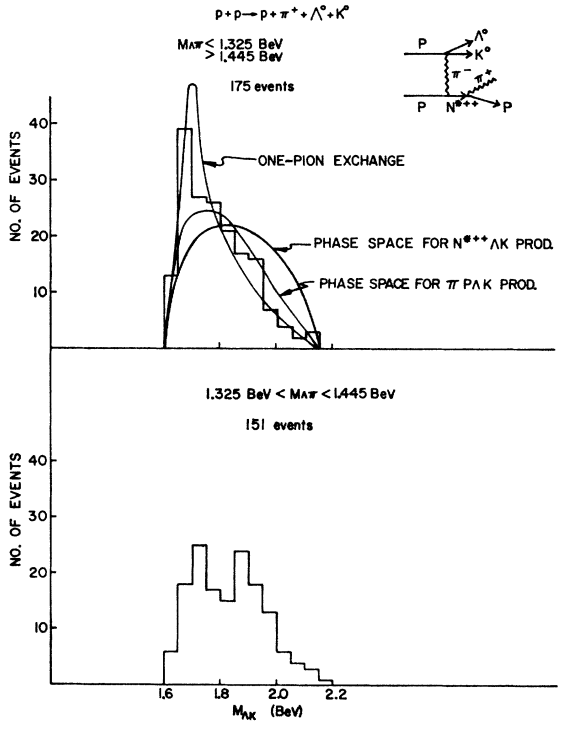

FIG. 15. Mass distribution of the hyperon-kaon system for events where an N^{*++} is produced and otherwise.

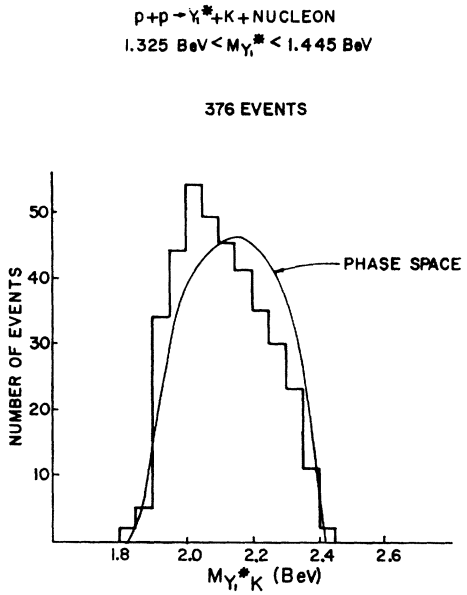

FIG. 16. Mass distribution of the Y_1^* K system in reactions (3), (4), (5), (7), and (8).

duction is most prominent for events whose $\Lambda\pi^+$ mass is outside the Y_1^* region.

The fits to the $\Lambda\pi^+$ mass distributions in Fig. 12 and the $p\pi^+$ mass distribution in Fig. 13 are very good fits to the data. The distributions used have the following form:

$$\frac{d\sigma}{dM}=a\frac{\Gamma/2}{(M-M_0)^2+\Gamma^2/4}\rho(M)+b\rho(M),$$

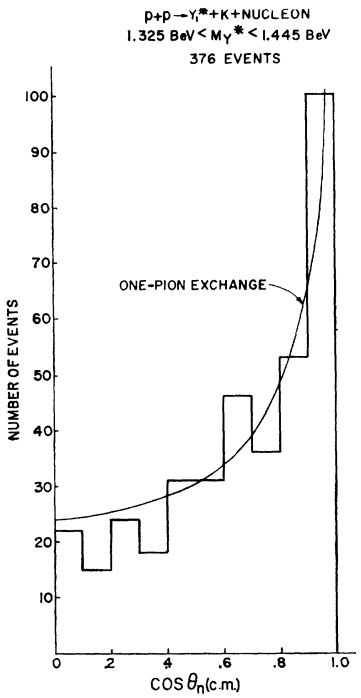

FIG. 17. Angular distribution of the nucleon in the production c.m. system in events where a Y_1^* is produced.

where $\rho(M)$ = phase space distribution normalized to the total number of events, $\frac{1}{2}\Gamma/[(M-M_0)^2+\Gamma^2/4]$ = the Breit-Wigner resonance matrix element squared,[16] a = constant that normalizes the distribution

$$\frac{\Gamma/2}{(M-M_0)^2+\Gamma^2/4}\rho(M)$$

to the total number of events that go through the resonant channel, b = constant that shows the fraction of events that do not go through the resonant channel.

The fits in Figs. (12) and (13) and the fact that the N^{*++} occurs mainly for non-Y_1^* events indicate that the reaction $p+p\to p+\pi^++\Lambda^0+K^0$ occurs mainly through two channels: namely, $p+p\to p+K^0+Y_1^{*+}$ and $p+p\to\Lambda^0+K^0+N^{*++}$. In Fig. 15 we show the mass of the ΛK system for those events in which the $\Lambda\pi^+$ mass combination is not a Y_1^* and otherwise. It is clear that the distribution is in reasonable agreement with the one pion exchange model.[17] Similarly, in Fig. 16 we show the mass distribution of the Y_1^*K combination. Again, there is a tendency of peaking towards low mass values. This is what one expects from one pion exchange. We do not draw any detailed curve since we do not know

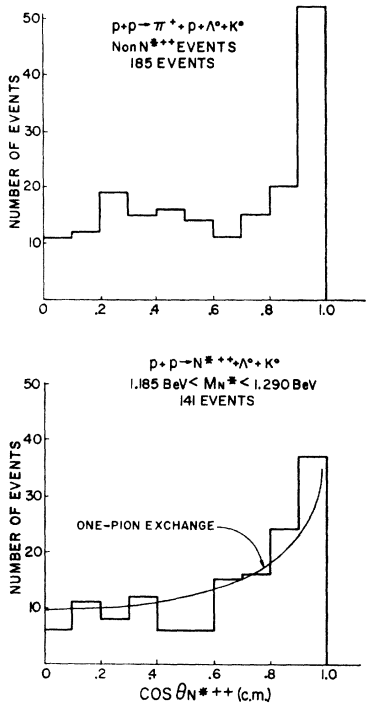

FIG. 18. Angular distribution of the N^{*++} in the production c.m. system in events where it is produced and for events where it is not produced.

[16] In this paper, we neglect the dependence of the width Γ on the mass and the spin of the resonance. This effect does not alter the fit to the data.

[17] In the application of the one-pion-exchange model to this resonance, we assume that the dynamical dependence of the $p\pi N^{*++}$ vertex is the same as that of the $p\pi p$ vertex in reaction (1) namely, Δ^2, the momentum transfer squared of the N^{*++} in one case and of the proton in the other.

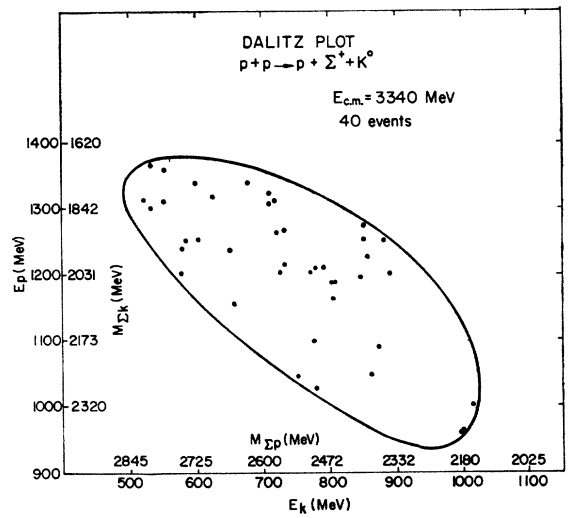

FIG. 19. Dalitz plot for reaction (10).

the energy dependence of Y_1^* K production in pion-nucleon collisions.

In Fig. 17 we show the angular distribution of the nucleon in the reaction $p+p \rightarrow Y_1^*+K^++$nucleon. Again, we have good agreement with the one pion exchange. Similarly, in Fig. 18 we have good agreement with the N^{*++} angular distribution. In both of these the angular distribution tends to be more peaked than predicted by the one-pion exchange. This is again expected if there is absorption in the incoming and outgoing channels.

In Fig. 19 we present the Dalitz plot for reaction (10). The events here also tend to have a low Σ-K mass similar to the reaction (2). This is in agreement with what one would expect from the one pion exchange model.

III. CONCLUSIONS

We were not able to detect any effect that could only be due to a dibaryon resonant state. All our data, including the total cross section in reaction (1) (which is the only cross section we can check), are consistent with the one-pion-exchange model. We observe the effects of the N^* ($I=\frac{1}{2}$) resonance at $M=1.69$ BeV in reaction (1). We observe a strong production of the Y_1^* resonance. We also observe the N^{*++} resonance.

We cannot verify the effects observed by Melissinos *et al.* and Wenzel[2] owing to our limited number of events.

ACKNOWLEDGMENTS

Our thanks are due to the crew of the Brookhaven 80-in. bubble chamber and the staff of the A. G. S. for their help and cooperation. We thank our scanning and measuring staff at Princeton for their excellent work in the analysis of the film. We would like to thank Ed Hart, R. Rau, and Virgil Barnes for their help in the determination of the bubble chamber constants. We thank D. Rahm, I. Skillicorn, and M. S. Webster who worked on the beam. Finally, we would like to thank Henry Blumenfeld and Maurice Bazin for their help in the initial stages of this experiment.